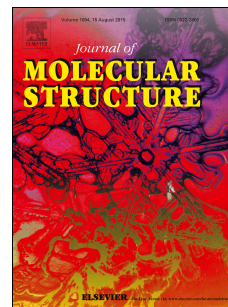


Accepted Manuscript

Structural considerations on acridine/acridinium derivatives: synthesis, crystal structure, Hirshfeld surface analysis and computational studies

Michał Wera, Piotr Storonik, Illia E. Serdiuk, Beata Zadykowicz



PII: S0022-2860(15)30343-4

DOI: [10.1016/j.molstruc.2015.10.041](https://doi.org/10.1016/j.molstruc.2015.10.041)

Reference: MOLSTR 21886

To appear in: *Journal of Molecular Structure*

Received Date: 6 July 2015

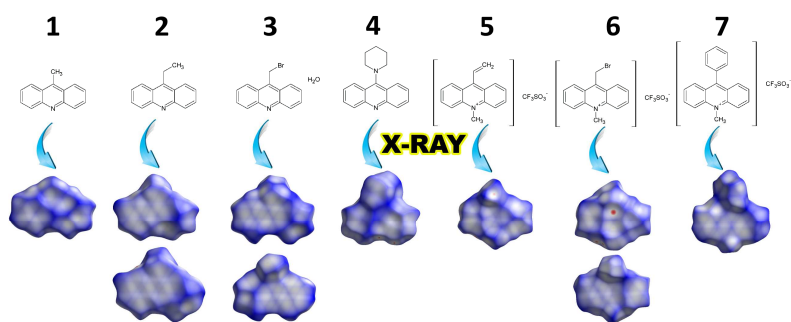
Revised Date: 21 September 2015

Accepted Date: 19 October 2015

Please cite this article as: M. Wera, P. Storonik, I.E. Serdiuk, B. Zadykowicz, Structural considerations on acridine/acridinium derivatives: synthesis, crystal structure, Hirshfeld surface analysis and computational studies, *Journal of Molecular Structure* (2015), doi: 10.1016/j.molstruc.2015.10.041.

This is a PDF file of an unedited manuscript that has been accepted for publication. As a service to our customers we are providing this early version of the manuscript. The manuscript will undergo copyediting, typesetting, and review of the resulting proof before it is published in its final form. Please note that during the production process errors may be discovered which could affect the content, and all legal disclaimers that apply to the journal pertain.

Graphical abstract



Structural considerations on acridine/acridinium derivatives: synthesis, crystal structure, Hirshfeld surface analysis and computational studies

Michał Wera^{*}, Piotr Storoniak, Illia E. Serdiuk, Beata Zadykowicz^{*}

Faculty of Chemistry, University of Gdańsk, Wita Stwosza 63, 80-308 Gdańsk, Poland

^{*} Corresponding author. Tel.: +48 58 523 51 13; fax: +48 58 523 50 12 (M. Wera, B. Zadykowicz);
E-mail address: michal.wera@ug.edu.pl (M. Wera); beata.zadykowicz@ug.edu.pl (B. Zadykowicz).

Abstract

This article describes a detailed study of the molecular packing and intermolecular interactions in crystals of four derivatives of acridine, i.e. 9-methyl-, 9-ethyl, 9-bromomethyl- and 9-piperidineacridine (**1**, **2**, **3** and **4**, respectively) and three 10-methylacridinium salts containing the trifluoromethanesulphonate anion and 9-vinyl-, 9-bromomethyl-, and 9-phenyl-10-methylacridinium cations (**5**, **6** and **7**, respectively). The crystal structures of all of the compounds are stabilized by long-range electrostatic interactions, as well as by a network of short-range C–H...O (in hydrates and salts **3** and **5–7**, respectively), C–H... π , π – π , C–F... π and S–O... π (in salts **5–7**) interactions. Hirshfeld surface analysis shows that various intermolecular contacts play an important role in the crystal packing, graphically exhibiting the differences in spatial arrangements of the acridine/acridinium derivatives under scrutiny here. Additionally, computational methods have been used to compare the intermolecular interactions in the crystal structures of the investigated compounds. Computations have confirmed the great contribution of dispersive interactions for crystal lattice stability in the case of 9-substituted acridine and electrostatic interactions for the crystal lattice stability in the case of 9-substituted 10-methylacridinium trifluoromethanesulphonates. The value of crystal lattice energy and the electrostatic contribution in the crystal lattice energy of monohydrated acridine derivatives have confirmed that these compounds have behave as acridinium derivatives.

Keywords Acridine and 10-methylacridinium derivatives · Crystal structure · Intra- and intermolecular interactions · Hirshfeld surface analysis

Introduction

Natural and synthetic acridine derivatives are among the oldest classes of bioactive agents. These compounds exhibit fungicidal, antimicrobial, anti-parasitic, anti-inflammatory, anticancer and antiviral activities [1–4]. Their anti-proliferative properties have been reported as well. Some acridine derivatives can bind DNA through intercalation [1], which leads to cell apoptosis. In addition, acridine-based derivatives have been studied as anticancer agents, which are believed to express their activity through the binding of DNA [2,5]. Similarly, 10-substituted acridinium derivatives, with a rigid aromatic tricyclic ring system, have been shown to possess potent chemo-sensitization pharmacophores [6].

On the other hand, an interesting group of acridine derivatives are those capable of chemiluminescence. This property is displayed by acridinium cations alkyl-substituted at the endocyclic nitrogen atom and containing electron-attracting substituents at C9. This latter atom is thus susceptible to the attack of anionic oxidants, e.g. hydrogen peroxide and persulphates [7–13]. Oxidation gives rise to electronically excited N-alkyl-9-acridinones; their relaxation is accompanied by the emission of light, i.e. chemiluminescence [7,8,10,11]. The efficiency of chemiluminescence, no greater than a few per cent [7,11], can be affected by the presence of various substances in the medium, including nucleophilic species, competing with oxidants for substitution at C9 [7,8,14]. This effect is utilized in the assay of oxidants, nucleophiles or other entities, and in such cases acridinium cations serve as chemiluminogenic indicators [7,9,14]. Acridinium chemiluminogens can also be linked by a spacer (e.g. an alkyl

chain) to an active group capable of reacting with appropriate fragments of macromolecules. Such chemiluminescent labels are widely used in chemical, medical, biological and environmental analyses [7–9,12].

We investigated the crystal structure as well as the intra- and intermolecular interactions of 10-methyl-9-phenoxyacetylacridinium derivatives [14–19] and 10-methyl-9-cyanoacridinium cations [20]. A disadvantage of these acridinium derivatives is the relatively inefficiency of their chemiluminescence. This encouraged us to search for new acridinium-based derivatives capable of reacting more efficiently with oxidizing agents to produce light. 9-Alkylacridine is the precursor of the 10-methyl-9-alkylacridinium cation, which displays a promising chemiluminogenic ability [21,22].

Intermolecular interactions, such as hydrogen bonds and π - π interactions, are of fundamental importance for supramolecular assembly and consequently for the properties of organic and inorganic compounds [23–25]. Self-assembly and molecular recognition processes of the compounds play a significant role in the context of their use as technological materials, drugs, or biologically active molecules [26–29]. Strong (O–H \cdots O and N–H \cdots O) and weak (C–H \cdots O) hydrogen bonding [30–35] remains the most reliable and widely used means of enforcing molecular recognition of crystalline materials. On the other hand, other weaker forces (π - π interactions) [29,32,36–39] have also been successfully utilized for such purposes. The increased interest in the understanding of the geometry, energies and nature of hydrogen bonding [30–35] and π - π interactions [29,32,36–39] in the past two decades, expressed primarily by the increasing number of publications on this topic, is understandable, given the enormous importance of these forces in building supramolecular self-assemblies.

In this paper, we report the results of the X-ray crystal structure determination of seven new 9-substituted acridine derivatives and 9-substituted-10-methylacridinium trifluoromethanesulphonates (Scheme 1). A comparative characterization of the title compounds is carried out, and details regarding the structural differences between them are discussed in the context of the intermolecular interactions present in the crystal state. In addition, intermolecular non-covalent interactions were studied using the Hirshfeld surface analysis [40–42]. In order to understand the nature of intra- and intermolecular interactions, we applied computational methods (CRYSTAL09 program at the DFT level of theory). The latter approach, the crystal lattice energies (E_L), together with the electrostatic (E_c) and dispersive contribution ($E(D^*)$) to the crystal lattice energy, and basis set superposition error energy correction (E_{BSSSE}) were calculated and interpreted.

Materials and methods

Synthesis

The chemicals were purchased from Sigma-Aldrich unless indicated otherwise. The purity of the compounds was checked by HPLC (Waters 600 E Multisolute Delivery System, Waters 2487 Dual λ Absorbance Detector; mobile phase: acetonitrile/water = 70%/30% supplemented with 0.1% of TFA; stationary phase: C-8 column, 3 \times 150mm, ‘Symmetry’) (the relative areas under the main signal were >99% in all cases) and their identity confirmed by mass spectrometry. The compounds obtained were subjected to elemental analyses (EAGER 200, Carlo Erba Instruments) and TLC tests in the above-mentioned system. ^1H spectra were recorded at room temperature on a Bruker AVANCE III 500 MHz.

9-Methylacridine (1). A mixture of 10 g of diphenylamine (59.1 mmol), acetic acid (10.0 mL), and anhydrous zinc chloride (40.0 g, 293.5 mmol) was heated at 220°C for 17 h. The reaction mixture was digested with hot 10% aqueous sulphuric acid and then strongly alkalinized with concentrated aqueous ammonia to dissolve the zinc chloride. The insoluble residue was extracted with toluene. The organic phase was washed with water (100 mL) and dried over sodium sulphate. After evaporation of the solvent, the crude product was purified by column chromatography (eluent *n*-hexane/ethyl acetate = 5/1 v/v). Yield 81 %; m.p. = 391 K; the % of elements found/calculated, C 86.93/87.01, H 5.74/5.74, N 7.09/7.25; ¹H NMR (CD₃CN), δ, ppm (J, Hz): 3.06 (3H, s); 7.52 (2H, t, J = 7.5); 7.71 (2H, t, J = 7.4); 8.04 (2H, d, J = 8.6); 8.28 (2H, d, J = 8.8).

9-Ethylacridine (2). A mixture of 0.17 g of diphenylamine (1 mmol), 1.1 ml propionic acid (15 mmol) and 0.46 g zinc chloride (3 mmol) was stirred and microwave-irradiated at 110°C and 120 W for 2h. The mixture was diluted with dichloromethane, washed with water, diluted with sodium hydroxide, washed again with water and dried over magnesium sulphate. After evaporation of the solvent, the crude product was purified by column chromatography (eluent 1–3% 2-propanol in chloroform). Yield 87 %; m.p. = 387 K; the % of elements found/calculated, C 86.69/86.92, H 6.34/6.32, N 6.71/6.76; ¹H NMR (CDCl₃), δ, ppm (J, Hz): 1.47 (3H, t, J = 7.7); 3.65 (2H, q, J = 7.7); 7.56 (2H, t, J = 7.7); 7.77 (2H, t, J = 8.0); 8.26 (4H, d, J = 8.8).

9-Bromomethylacridine (3) was synthesized according to the procedure described in [43]. Yield 77 %; m.p. = 443 K; the % of elements found/calculated, C 61.26/61.79, H 3.64/3.70, N 5.03/5.15; ¹H NMR (CDCl₃), δ, ppm (J, Hz): 5.38 (2H, s); 7.62 (2H, t, J = 7.7); 7.78 (2H, t, J = 7.7); 8.31 (4H, d, J = 8.8).

9-Piperidylacridine (4). 0.213 g (1.0 mmol) of 9-chloroacridine hydrochloride was dissolved in 2 ml piperidine and heated to 90°C with constant stirring for 6 h. The solvent was evaporated under vacuum at 50°C. The residue was washed with aqueous methanol and dried in a vacuum. Yield 91 %; m.p. = 383 K; the % of elements found/calculated, C 81.96/82.41, H 7.01/6.92, N 10.93/10.68; ¹H NMR (CDCl₃), δ, ppm (J, Hz): 1.80 (2H, m); 1.84 (4H, m); 3.59 (4H, m); 7.38 (2H, t, J = 7.6); 7.64 (2H, t, J = 7.6); 8.15 (2H, d, J = 8.6); 8.28 (2H, d, J = 8.9).

General procedure for the synthesis of 10-methylacridinium trifluoromethanesulphonate derivatives To a solution of 1 mmol of an acridine derivative in 10 ml dry dichloromethane were added 4 mmol 2,6-ditert-butylpyridine and 5 mmol methyl trifluoromethanesulphonate. The solution was stirred at room temperature for 3 h. The precipitate was filtered off and washed with dichloromethane. The filtrate was evaporated under vacuum at room temperature to 5 ml and diluted with diethyl ether. The precipitate was filtered and vacuum-dried.

10-Methyl-9-vinyl-acridinium trifluoromethanesulphonate (5). First, we synthesized the precursor of 10-methyl-9-vinylacridinium trifluoromethanesulphonate – 9-vinylacridine – following the procedure described below. To a suspension of 0.535 g (1.5 mmol) triphenylmethylphosphonium bromide in 10 ml dry diethylether was added 0.168 g (1.5 mmol) of potassium *tert*-butylate and stirred for 30 min. Then 0.207 g (1.0 mmol) acridine-9-carboxaldehyde was added and the mixture stirred at ambient temperature overnight. After dilution with 50 ml dichloromethane, the solution was washed with water three times, after which the organic layer was separated, dried over magnesium sulphate and evaporated to dryness. The target compound was purified by column chromatography (eluent 1% 2-propanol in chloroform). Yield 73 %; m.p. = 350 K; the % of elements found/calculated, C 87.27/87.77, H 5.66/5.40, N 6.48/6.82; ¹H NMR (CDCl₃), δ, ppm (J, Hz): 5.60 (1H, d, J = 11.8); 5.98 (1H, d, J = 11.8); 7.32 (1H, dd, J = 11.8);

7.39 (2H, t, J = 7.5); 7.65 (2H, t, J = 7.5); 8.13 (4H, d, J = 8.9). Pure 9-vinylacridine was converted to 10-methylacridinium derivatives according to the general procedure for synthesizing 10-methylacridinium trifluoromethanesulphonate derivatives described above. Yield 83 %; m.p. = 442 K; $^1\text{H NMR}$ (CD_3CN), δ , ppm (J, Hz): 4.78 (3H, s); 5.94 (1H, d, 17.5); 6.46 (1H, d, 11.8); 7.80 (1H, m); 7.97 (2H, m); 8.42 (2H, m); 8.58 (2H, d, J = 8.4); 8.74 (2H, d, J = 7.7).

9-Bromomethyl-10-methylacridinium trifluoromethanesulphonate (6). Yield 87 %; m.p. = 487 K; $^1\text{H NMR}$ (CD_3CN), δ , ppm (J, Hz): 4.79 (3H, s); 5.73 (2H, s); 8.10 (2H, t, J = 7.3); 8.43 (2H, t, J = 7.3); 8.63 (2H, d, J = 9.2); 8.81 (2H, d, J = 8.7).

10-Methyl-9-phenyl-acridinium trifluoromethanesulphonate (7). Yield 79 %; $^1\text{H NMR}$ (CD_3CN), δ , ppm (J, Hz): 4.87 (3H, s); 7.62 (1H, d, 8.8); 7.78 (2H, m); 7.89 (4H, m); 8.07 (2H, d, 8.8); 8.40 (2H, t, 7.6); 8.65 (2H, d, J = 8.8).

Crystals suitable for X-ray investigations were grown by slow evaporation of dichloromethane in the case of **1**, **3**, **4**, **5**, **6** and **7** and dichloromethane:acetonitrile (1:1 v/v) solution in the case of **2**.

Single crystal X-ray diffraction analysis

Crystallographic data were collected on an Oxford Diffraction Gemini R Ultra Ruby CCD diffractometer with graphite-monochromatic Cu- K_α radiation ($\lambda = 1.54184 \text{ \AA}$) at 295 K. Data sets were collected using the ω scan technique. The CrysAlis CCD [44] and CrysAlis RED [45] programs were used for data collection, cell refinement and data reduction, and a multi-scan absorption correction was applied. Crystal data and details concerning the structural refinement are given in Table 1.

Structures were solved by direct methods using SHELXS-97 [46]. The initial model was refined by the full-matrix least squares method on F^2 with SHELXL2013 [47], adopting anisotropic thermal parameters for non-hydrogen atoms. The H-atoms of the water molecules were located on a Fourier-difference map, restrained by DFIX command 0.85 for O–H distances and by DFIX 1.39 for H...H distance and refined as riding with $U_{\text{iso}}(\text{H}) = 1.5U_{\text{eq}}(\text{O})$. All other hydrogen atoms were positioned stereochemically and refined with fixed individual isotropic displacement parameters [$U_{\text{iso}}(\text{H}) = 1.2U_{\text{eq}}(\text{C}_{\text{sp}}^2)$ or $1.5U_{\text{eq}}(\text{C}_{\text{sp}}^3)$] using a riding model with C–H bond lengths of either 0.93 \AA (C_{sp}^2) or 0.96 \AA (methyl C_{sp}^3) and 0.97 \AA (non-methyl C_{sp}^3).

ORTEP-3 [48] software was used to prepare the molecular graphics and the PLATON [49] and CrystalExplorer 3.1 [50] programs to reveal and analyse the molecular interactions.

Computational details

Calculations were carried out using the periodic *ab initio* CRYSTAL09 program [51] at the density functional theory (DFT) level [52], using the B3LYP functional [53–55] and 6-31G** basis sets [56,57]. For a given experimental crystal structure, single point calculations of periodic wave function and energy were performed. Using calculated total energies, being the sum of electronic and nuclear repulsion energy, the cohesive energy of the crystal can be obtained according to the following formula [58]:

$$E_c = \frac{E_{\text{bulk}}}{Z} - E_{\text{mol}}$$

where E_{bulk} is the total energy of the unit cell, Z is the number of molecules in the unit cell, and E_{mol} is the total energy of the molecule extracted from the bulk. The *ab initio* DFT total energy values obtained, were subsequently corrected to take into account dispersive interactions. Here, we employed empirically modified Grimme dispersion correction proposed by Civalleri et al. for molecular crystals (model in the original work referred to as B3LYP-D*) [58].

In order to avoid overestimation of the strength of interactions within crystals, cohesive energies E_c were additionally corrected for basis set superposition error by the counterpoise method [59] implemented in the CRYSTAL09 code. Final theoretical lattice energy, E_L , from CRYSTAL09 calculation comprises of three terms:

$$E_L = E_c + E(D^*) + E_{\text{BSSE}}$$

Theoretical cohesive energies E_L may be compared with lattice energies obtained from experimental sublimation enthalpies.

Calculations of the atomic point charges on nitrogen (N10) atom, necessary for prediction of the electrostatic energy interactions were carried out at the DFT level [52] by reproducing the electrostatic potential around molecules (ESP fit charges) [60]. In these calculations the M06-2X [31,61] functional was employed together with the 6-31++G** basis set [62]. Calculations were carried out using the Gaussian 09 program [63].

Results and discussion

Molecular and crystal structure

In the target compound molecules, the bond lengths and angles characterizing the geometry of the acridine rings (**1–4**) and the acridinium moieties (**5–7**) (Table 1, Scheme 1) are typical of unmethylated [19,64] and methylated [65–67] acridine-based derivatives.

The asymmetric unit in acridines consists of one (**1** and **4**) or two (**2** and **3**) crystallographically independent acridine molecules (A and B) (Figs 1 a–d). The asymmetric unit of **3** also contains two water molecules. In the acridinium salts the asymmetric unit consists of one (**5** and **7**) or two (**6**) crystallographically independent ion pairs (Figs 1 e–g).

In acridines unmethylated at the N10 position (**1–4**) the rings 1, 2 and 3 are all planar with a small dihedral angle between rings 3 and 2 (Scheme 2, Table 1S in Supplementary material), creating a planar acridine core except for compound **4**, whose dihedral angle is significantly larger at 4.1 (2)°. In the methylated acridines (**5–7**) the RMS deviations from planarity for ring 1 are slightly higher and the dihedral angle between rings 3 and 2 varies from 3.4 (1) to 9.3 (2)°, causing the acridinium core to be distorted.

In compound **4** (Fig. 1d) atoms C16 and C19 of the piperidine fragment occupy two positions in the crystalline solid phase, with occupancy factors of 0.828(4) and 0.172(4) for C16/C19 and C16X/C19X, respectively. The piperidine ring 4 (N15/C16–C20) is not planar, having a total puckering amplitude, Q_T , of 0.545(2) Å and a conformation resembling a chair [$\varphi = 64(3)^\circ$ and $\theta = 3(1)^\circ$]; the disordered ring 4 (N15/C16X/C17–C18/C19X/C20) is not planar either, with a total puckering amplitude, Q_T , of 0.270(8) Å [$\varphi = 7(1)^\circ$ and $\theta = 131(11)^\circ$] [68]. The

following discussion and interaction calculations take only the major disordered part into account. The piperidine ring 4 is twisted at an angle of $60.0(1)^\circ$ relative to the acridine skeleton.

Ring 4 in 10-methyl-9-phenylacridinium trifluoromethanesulphonate (**7**) is planar and twisted relative to the acridine skeleton at an angle of $68.1(1)^\circ$.

The structural analysis carried out with aid of PLATON revealed various types of intra- and intermolecular interactions in the crystal lattices of the target compounds. These are listed in Tables 2–4 and illustrated in Figs 1 and 2. The molecules in all the crystal structures of these compounds are involved in π – π contacts (Table 3) [36]. Strong hydrogen bonds of types O–H \cdots O and O–H \cdots N (Table 2, Figs 1 and 2) [30] occur only in the crystal structure of **3**, owing to the presence of water molecules. Weak hydrogen bonds like C–H \cdots O [31,69] (**2**, **3**, **5**, **6** and **7**) and C–H \cdots π [70] (**4**) occur as well (Table 2, Fig. 2). Furthermore, other interactions like S–O \cdots π (**5**, **6** and **7**) [32] and C–F \cdots π [32] (**5** and **6**) are present in the crystal structure of acridinium salts (Table 4, Figs 1 and 2).

Compounds **1** and **3** crystallize in the orthorhombic crystal system and in the $P2_12_12_1$ space group. In the crystal structure of **1** aromatic rings 2 and 3 are involved in π – π contacts (Table 3) [36] between two parallel oriented molecules, creating columns along the a axis (Fig. 3). Molecules in adjacent columns are inclined at angles of $51.4(1)$, $62.4(1)$ and $85.0(1)^\circ$. In the asymmetric unit of **3** molecules A and B of the title compound are inclined at an angle of $77.3(2)^\circ$. In the crystal structure molecules A and B of **3** are linked via a hydrogen bonding bridge (of types O–H \cdots O and O–H \cdots N) [30] via two water molecules forming chains along the a axis, and stabilized through multidirectional π – π contacts (Table 3, Fig. 2) [36] in columns of homonymous molecules. Moreover, a weak C–H \cdots O (Table 2, Fig. 2) [31,69] hydrogen bond links adjacent chains along the b axis. Homonymous molecules in the columns are parallel. Molecules A and A in adjacent columns are inclined at an angle of $31.7(2)^\circ$, molecules B and B at $38.5(2)^\circ$ and molecules A and B at $87.8(2)^\circ$.

Compounds **2**, **5** and **7** crystallize in the monoclinic crystal system. For **2** the space group is $P2_1/c$. In the asymmetric unit, molecules A and B of **2** are inclined at an angle of $73.4(2)^\circ$. Two A molecules in the crystal structure are connected by π – π (Table 3, Fig. 2) [36] contacts forming dimers, and two B molecules also form dimers via π – π (Table 3, Fig. 2) [36] contacts. Additionally, B molecules from adjacent dimers are connected by a weak C–H \cdots O type hydrogen bond (Table 2, Fig. 2) [31,69]. Homonymous molecules assemble into layers parallel to the (100) plane. Molecules A in dimers are parallel and inclined in adjacent dimers at an angle of $89.8(2)^\circ$. Molecules B in dimers are parallel and inclined in adjacent dimers at an angle of $88.6(2)^\circ$. In adjacent dimers molecules A and B are inclined at an angle of $73.4(2)$ or $45.4(3)^\circ$. Molecules A and B produce two independent herringbone patterns, rotated by $73.4(2)^\circ$, in the crystal structure of **2** (Fig. 3). A herringbone pattern also occurs in the crystal lattice of **5** and **7**, where the mean planes of the adjacent acridinium moieties are parallel or inclined at angles of $18.2(1)^\circ$ in **5** and $65.8(1)^\circ$ in **7** (Fig. 3). In the crystal structure of **5** two cations are linked by π – π (Table 3, Fig. 2) [36] contacts forming dimers connected to anions via C–H \cdots O (Table 2, Fig. 2) [31,69], S–O \cdots π (Table 4, Fig. 2) [32] and C–F \cdots π (Table 4, Fig. 2) [30] interactions. In the crystal structure of **7** ion pairs are linked by weak C–H \cdots O type hydrogen bonds (Table 2, Fig. 2) [31,69]. The adjacent cations are linked by π – π (Table 3, Fig. 2) [36] contacts forming layers (parallel to (20-2) and the neighbouring cations and anions via C–H \cdots O (Table 2, Fig. 2) [31,69] and S–O \cdots π (Table 4, Fig. 2) [32] interactions.

Compounds **4** and **6** crystallize in the triclinic crystal system and in the P-1 space group. The molecules in the crystal structure of both **4** and **6** are parallel and involved in π - π contacts. In **4** these contacts between aromatic rings 1, 2 and 3 of two inversely oriented molecules form dimers linked via a weak C—H $\cdots\pi$ (Table 2, Fig. 2) [70] hydrogen bond, in turn forming columns along the b axis (Fig. 3). The ion pairs in the crystal structure of **6** are linked by S—O $\cdots\pi$ (Table 4, Fig. 2) [32] and C—F $\cdots\pi$ (Table 4, Fig. 2) [30] interactions, and cations A and B are linked by π - π (Table 3, Fig. 2) [36] contacts, thereby forming dimers connected to anions from adjacent dimers via C—H \cdots O (Table 2, Fig. 2) [31,69] interactions.

The crystal structure of acridinium salts (**5–7**) is stabilized by a network of the above-mentioned specific short-range interactions and by long-range electrostatic interactions between ions. Analysis of the packing of acridinium salts reveals the formation of layers of cations and anions (Fig. 4).

Hirshfeld analysis

In order to profoundly examine the strength and role of the above listed hydrogen bonds and other intermolecular contacts, and to estimate their importance for the crystal lattice stability, Hirshfeld surface analysis and computational study have been conducted. Comprehensive analysis of Hirshfeld surfaces (Figs 5 and 1S in Supplementary material), the associated fingerprint plots [71,72] (Figs 6 and 2S in Supplementary material) and the percentage contributions of various close intermolecular contacts to the Hirshfeld surface area (Fig. 7) generated with the CrystalExplorer 3.1 program [50], carried out in accordance with the rules outlined in the literature and the examples described [40,41], confirms the occurrence of the interactions revealed by PLATON [49] and listed in Tables 2–4.

The two-dimensional (d_e/d_i) fingerprint plots exhibit significant differences resulting from the interactions occurring in the crystal lattice of the target compounds (Figs 6 and 7 and 2S in Supplementary material). A quite high contribution of H \cdots H contacts to the total Hirshfeld surface of all acridine and acridinium moieties is common in organic molecular crystals. All acridine and acridinium moieties are involved in π - π contacts, which is confirmed by the presence of light-green areas of the C \cdots C contributions to the Hirshfeld surface. An intermolecular C—H $\cdots\pi$ interaction (Table 2) is involved in molecule **2B**: surprisingly, however, the presence of such an interaction is not evident and the contributions of H \cdots C and C \cdots H contacts of both crystallographically independent molecules are similar. This is not the case for compound **4**, in which the H \cdots C and C \cdots H fingerprint plot exhibits the presence of wings associated with weak C—H $\cdots\pi$ interactions. For **3** the conspicuous presence of strong O—H \cdots N hydrogen bonds in both crystallographically independent molecules is marked by the occurrence of long spikes with the contribution of H \cdots N and N \cdots H contacts to the total Hirshfeld surface of 4.0% and 3.7% for molecules **A** and **B**, respectively. Since the weak C—H \cdots O hydrogen bond involves only the **3B** molecule its existence is indicated by a small spike with a contribution of H \cdots O and O \cdots H contacts of 4.2%. Such distinctive spikes associated with weak intermolecular C—H \cdots O hydrogen bonds are also present in the fingerprint plots of **5**, **6A**, **6B** and **7**, with respective contributions of 17.8%, 16.4%, 16.2% and 15.4%. The contribution of C \cdots O and O \cdots C contacts to the total Hirshfeld surface, ascribed to S—O $\cdots\pi$ contacts, is relatively small (3.6%, 2.9%, 3.9% and 1.4% for **5**, **6A**, **6B** and **7**, respectively) for interactions between oppositely charged ions. The F \cdots C and C \cdots F contacts denote the existence of C—F $\cdots\pi$

interactions involving molecules **5** and **6** with contribution of 4.5% and 2.5%, respectively. Due to the high proportion of hydrogen atoms in relation to the non-hydrogen atoms in a molecule and their presence in the most outer fragments of the molecule, it is understandable that their contribution to the Hirshfeld surfaces is significant.

Crystal lattice energies

The crystal lattice energies (E_L), which are important thermodynamic characteristics of crystalline substances, calculated for all compounds, together with the electrostatic contribution calculated from the difference in electronic and nuclear repulsion energy of bulk crystal and molecules in the bulk (E_c), and dispersive contribution derived from modified Grimme model ($E(D^*)$) to the crystal lattice energy, are shown in Table 5. The crystal lattice energy values are corrected for the value of basis set superposition error energy correction (E_{BSSE}), which are less than 4.0 kJ mol^{-1} in the case of 9-substituted acridine (**1,2,4**) and between 94.8 and 98.1 kJ mol^{-1} in the case of 9-substituted 10-methylacridinium trifluoromethanesulphonates (**5–7**). Basis set superposition error energy correction values (E_{BSSE}) for 9-bromomethylacridine monohydrate (**3**) are higher than in the other investigated 9-substituted acridine (**1,2,4**) (62.9 kJ mol^{-1}). The crystal lattice energies and their electrostatic and dispersive contributions of 9-substituted acridine and their 9-substituted 10-methylacridinium trifluoromethanesulphonates (Table 5) are typical of acridine derivatives and their salts containing complex monovalent ions [73,74]. Only in the case of 9-bromomethylacridine monohydrate (**3**), the crystal lattice energy and the electrostatic contribution in the crystal lattice energy are significantly higher than in the other investigated 9-substituted acridine (**1, 2, 4**). Following these results, we investigated ESP fitted atomic partial charges on N10 atom of the acridine/acridinium derivatives using two methods: first, where atomic partial charges were calculated for all atoms of the electroneutral asymmetric unit, and second, where atomic partial charges were calculated separately for molecules in the unit cell (assuming charge +1 for acridinium molecule and -1 for trifluoromethanesulphonate counterpart). The value of atomic partial charges on N10 atom is ca. 5 times lower in the case of 9-substituted acridines than in the case of 10-methylacridinium trifluoromethanesulphonates (Table 5). The value of the atomic partial charges on N10 atom of 9-bromomethylacridine monohydrate is ca. 3 times higher than in the case of others investigated 9-substituted acridines (-0.25 and -0.74 , respectively; the second value is average for **1, 2** and **4**), where the atomic partial charges were calculated for all atoms of the electroneutral asymmetric unit. When atomic partial charges were calculated separately for molecules in the unit cell, the value of the atomic partial charges on N10 atom of 9-bromomethylacridine monohydrate (**3**) was similar to the value of the atomic partial charges on N10 atom of others investigated 9-substituted acridines (**1, 2** and **4**). Taking into account general chemical knowledge, as well as the information mentioned above, we consider that monohydrated acridine derivatives behave as acridinium derivatives or acid–base pair. Therefore, the crystal lattice energy, the electrostatic contribution in the crystal lattice energy and the basis set superposition error energy correction of 9-bromomethylacridine monohydrate (**3**) are higher than in non-monohydrated acridine derivatives (**1, 2, 4**).

Knowing the crystal lattice energy, the electrostatic and dispersive contributions to the values of this quantity can be found. As the data in Table 5 demonstrates, the main contribution to the crystal lattice energy of 9-substituted acridine is from dispersive interactions, and that of 9-substituted 10-methylacridinium

trifluoromethanesulphonates from electrostatic interactions. Therefore, theoretical analysis shows that the cohesive forces in acridine derivatives (**1–4**) and in 10-methylacridinium salts (**5–7**) are of different origin.

Conclusion

Four derivatives of acridine, i.e. 9-methyl-, 9-ethyl, 9-bromomethyl- and 9-piperidineacridine and three 10-methylacridinium salts containing the trifluoromethanesulphonate anion and 9-vinyl-, 9-bromomethyl, and 9-phenyl-10-methylacridinium cations were obtained and structurally characterized.

The molecular arrangement in the crystals revealed that hydrogen bonds and van der Waals contacts play a significant part in intermolecular interactions. The crystal structures of all of the target compounds are stabilized by long-range electrostatic interactions, as well as by a network of short-range C–H \cdots O (in hydrates and salts, **3** and **5–7**, respectively), C–H \cdots π , π – π , and C–F \cdots π as well as S–O \cdots π (in salts **5–7**) interactions. Hirshfeld surface analysis shows that various intermolecular contacts play an important role in the crystal packing, revealing graphically the differences in spatial arrangements of the investigated acridine/acridinium derivatives.

Computational methods have confirmed that crystal lattice energies and their electrostatic and dispersive contributions of 9-substituted acridine and their 9-substituted 10-methylacridinium trifluoromethanesulphonates (Table 5) are typical of acridine derivatives and their salts containing complex monovalent ions (ca. -140 and -530 kJ mol $^{-1}$, respectively). Computations have confirmed the great contribution of dispersive interactions for the crystal lattice stability in the case of 9-substituted acridine and electrostatic interactions for the crystal lattice stability in the case of 9-substituted 10-methylacridinium trifluoromethanesulfonates. The value of crystal lattice energy, the electrostatic contribution in the crystal lattice energy of monohydrated acridine derivatives have confirmed that these compounds behave as acridinium derivatives.

An interesting aspect of the structural studies would be to correlate the structural parameters with the physicochemical properties (obtained experimentally or computationally) of the target compounds. The correlations would enable compounds with analytically interesting properties to be modelled. To shed more light on this issue, however, it will be necessary to investigate the luminescent (fluorescent and/or chemiluminescent) properties of the title compounds. This particular problem is one that we are currently investigating.

Supplementary data

Complete X-ray data have been deposited with the Cambridge Crystallographic Data Centre (CCDC) as supplementary publications Nos. 1058681–1058687; copies of these data can be obtained, free of charge, on application to CCDC, 12 Union Road, Cambridge CB2 1EZ, UK (fax: +44-(0)1223-336033 or e-mail: deposit@ccdc.cam.ac.uk).

Acknowledgements This study was financed from the State Funds for Scientific Research through an NSC grant 2011/03/D/ST4/02419 (contract No. UMO-2011/03/D/ST4/02419). Calculations were carried out on the computers of the Wrocław Centre for Networking and Supercomputing (WCSS) (grants no. 196 and 215). This publication

reflects the views only of the authors: the sponsor cannot be held responsible for any use which may be made of the information contained herein.

References:

- [1] W.A. Denny, *Curr. Med. Chem.* 9 (2002) 1655–1665.
- [2] K. Dzierzbicka, A.M. Kołodziejczyk, B. Wysocka-Skrzela, A. Myśliwski, A.D. Sosnowska, *J. Med. Chem.* 44 (2001) 3606–3615.
- [3] M. Kukowska-Kaszuba, K. Dzierzbicka, M. Serocki, A. Składanowski, *J. Med. Chem.* 54 (2011) 2447–2454.
- [4] M. Małachowska-Ugarte, G. Cholewiński, K. Dzierzbicka, P. Trzonkowski, *Eur. J. Med. Chem.* 54 (2012) 197–201.
- [5] T. Bentin, P.E. Nielsen, *J. Am. Chem. Soc.* 125 (2003) 6378–6379.
- [6] J.X. Kelly, M.J. Smilkstein, R.A. Cooper, K.D. Lane, R.A. Johnson, A. Janowsky, R.A. Dodean, D.J. Hinrichs, R. Winter, M. Riscoe, *Antimicrob. Agents Chemother.* 51 (2007) 4133–4140.
- [7] L.J. Kricka, *Anal. Chim. Acta* 500 (2003) 279–286.
- [8] C. Dodeigne, L. Thunus, R. Lejeune, *Talanta* 51 (2000) 415–439.
- [9] A. Roda, M. Guardigli, *Anal. Bioanal. Chem.* 402 (2012) 69–76.
- [10] J. Rak, P. Skurski, J. Błażejowski, *J. Org. Chem.* 64 (1999) 3002–3008.
- [11] K. Krzymiński, A. Ozóg, P. Malecha, A.D. Roshal, A. Wróblewska, B. Zadykowicz, J. Błażejowski, *J. Org. Chem.* 76 (2011) 1072–1085.
- [12] A. Natrajan, D. Sharpe, J. Costello, Q. Jiang, *Anal. Biochem.* 406 (2010) 204–213.
- [13] A. Natrajan, D. Sharpe, D. Wen, *Org. Biomol. Chem.* 10 (2012) 3432–3447.
- [14] J. Meszko, K. Krzymiński, A. Konitz, J. Błażejowski, *Acta Cryst. C*58 (2002) o157–o158.
- [15] A. Sikorski, K. Krzymiński, A. Konitz, J. Błażejowski, *Acta Cryst. C*61 (2005) o50–o52.
- [16] D. Trzybiński, A. Ozóg, K. Krzymiński, J. Błażejowski, *Acta Cryst. E*68 (2012) o625–o626.
- [17] D. Trzybiński, A. Sieradzan, K. Krzymiński, J. Błażejowski, *Acta Cryst. E*68 (2012) o1722–o1723.
- [18] D. Trzybiński, M. Wera, K. Krzymiński, J. Błażejowski, *Acta Cryst. E*69 (2013) o166.
- [19] M. Wera, D. Trzybiński, K. Krzymiński, J. Błażejowski, *Acta Cryst. E*69 (2013) o305.
- [20] O.M. Huta, I.O. Patsaj, A. Konitz, J. Meszko, J. Błażejowski, *Acta Cryst. C*58 (2002) o295–o297.
- [21] F. McCapra, I. Behesti, A. Burford, R.A. Hann, K.A. Zaklika, *J. Chem. Soc. Chem. Commun.* (1977) 944–948.
- [22] K. Papadopoulos, J. Lignos, M. Stamatakis, D. Dimotikali, J. Nikokavouras, *J. Photochem. Photobiol. A: Chem.* 115 (1998) 137–142.
- [23] G.R. Desiraju, *Angew. Chem., Int. Ed. Engl.* 34 (1995) 2311–2327.
- [24] D. Braga, F. Grepioni, *Making Crystals by Design: Methods, Techniques and Applications*, Wiley-VCH, Weinheim, 2007.
- [25] C.B. Aakeröy, J. Desper, B.M.T. Scott, *Chem. Commun.* (2006) 1445–1447.
- [26] J.Y. Lee, B.H. Hong, W.Y. Kim, S.K. Min, Y. Kim, M.V. Jouravlev, R. Bose, K.S. Kim, I.C. Hwang, L.J. Kaufman, C.W. Wong, P. Kimand, K.S. Kim, *Nature* 460 (2009) 498–501.
- [27] B.H. Hong, S.C. Bae, C.W. Lee, S. Jeong, K.S. Kim, *Science* 294 (2001) 348–351.

- [28] B.H. Hong, J.Y. Lee, C.W. Lee, J.C. Kim, S.C. Bae, K.S. Kim, *J. Am. Chem. Soc.* 123 (2001) 10748–10749.
- [29] S.K. Seth, D. Sarkar, T. Kar, *CrystEngComm* 13 (2011) 4528–4535.
- [30] G.R. Desiraju, *Acc. Chem. Res.* 35 (2002) 565–573.
- [31] Y. Zhao, D.G. Truhlar, *Acc. Chem. Res.* 41 (2008) 157–167.
- [32] T. Dorn, C. Janiak, K. Abu-Shandi, *CrystEngComm* 7 (2005) 633–641.
- [33] A.C. Cunha, V.F. Ferreira, A.K. Jordão, M.C.B.V. de Souza, S.M.S.V. Wardell, J.L. Wardell, P.A. Tan, R.P.A. Bettens, S.K. Seth, E.R.T. Tiekink, *CrystEngComm* 15 (2013) 4917–4929.
- [34] S.K. Seth, *Inorg. Chem. Comm.* 43 (2014) 60–63.
- [35] S.K. Seth, V.S. Lee, J. Yana, S.M. Zain, A.C. Cunha, V.F. Ferreira, A.K. Jordão, M.C.B.V. de Souza, S.M.S.V. Wardell, J.L. Wardell, E.R.T. Tiekink, *CrystEngComm* 17 (2015) 2255–2266.
- [36] E.R.T. Tiekink, J. Zukerman-Schpector, *The Importance of Pi-Interactions in Crystal Engineering: Frontiers in Crystal Engineering*, John Wiley & Sons, Ltd, Chichester, 2012.
- [37] S.K. Seth, P. Manna, N.J. Singh, M. Mitra, A.D. Jana, A. Das, S.R. Choudhury, T. Kar, S. Mukhopadhyay, K.S. Kim, *CrystEngComm* 15 (2013) 1285–1288.
- [38] P. Manna, S.K. Seth, M. Mitra, A. Das, N.J. Singh, S.R. Choudhury, T. Kar, S. Mukhopadhyay, *CrystEngComm* 15 (2013) 7879–7886.
- [39] P. Manna, S.K. Seth, M. Mitra, S.R. Choudhury, A. Bauzá, A. Frontera, S. Mukhopadhyay, *Cryst. Growth Des.* 14 (2014) 5812–5821.
- [40] J.J. McKinnon, M.A. Spackman, A.S. Mitchell, *Acta Cryst.* B60 (2004) 627–668.
- [41] P. Panini, T.P. Mohan, U. Gangwar, R. Sankolli, D. Chopara, *CrystEngComm* 15 (2013) 4549–4564.
- [42] S.K. Seth, D. Sarkar, A.D. Jana, T. Kar, *Cryst. Growth Des.* 11 (2011) 4837–4849.
- [43] W. Yang, Y. Wong, O.T.W. Ng, H.W. Li, K.K.L. Yung, D.W.J. Kwong, R.M.S. Wong, US Patent US2012/0269738A1, 2012.
- [44] Oxford Diffraction, CrysAlis CCD, Oxford Diffraction Ltd, Yarnton, England, 2008.
- [45] Oxford Diffraction, CrysAlis RED, Oxford Diffraction Ltd, Yarnton, England, 2008.
- [46] G.M. Sheldrick, *Acta Cryst.* A64 (2008) 112–122.
- [47] G.M. Sheldrick, SHELXL2013, University of Göttingen, Germany, 2013.
- [48] L.J. Farrugia, *J. Appl. Cryst.* 30 (1997) 565.
- [49] A.L. Spek, *Acta Cryst.* D65 (2009) 148–155.
- [50] S.K. Wolff, D.J. Grimwood, J.J. McKinnon, M.J. Turner, D. Jayatilaka, M.A. Spackman, *CrystalExplorer* (Version 3.1), University of Western Australia, 2012.
- [51] R. Dovesi, V.R. Saunders, C. Roetti, R. Orlando, C.M. Zicovich-Wilson, F. Pascale, B. Civalleri, K. Doll, N.M. Harrison, I.J. Bush, P. D’Arco, M. Llunell, CRYSTAL09, Università di Torino, Torino, Italy, 2009.
- [52] J.K. Labanowski, in: *Density Functional Methods in Chemistry*, ed. J. W. Andzelm, Springer-Verlag, New York, 1991.
- [53] A.D. Becke, *J. Chem. Phys.* 98 (1992) 9173–9177.
- [54] A.D. Becke, *J. Chem. Phys.* 98 (1993) 5648–5652.
- [55] C. Lee, W. Yang, R. G. Parr, *Phys. Rev. B* 37 (1988) 785–789.

- [56] P.C. Hariharan, J.A. Pople, *Theor. Chim. Acta* 28 (1973) 213–222.
- [57] W.J. Hehre, L. Radom, P.vR. Schleyer, J.A. Pople, *Ab Initio Molecular Orbital Theory*, Wiley, New York, 1986.
- [58] B. Civalleri, C.M. Zicovich-Wilson, L. Valenzano, P. Ugliengo, *CrystEngComm* 10 (2008) 405–410.
- [59] S.F. Boys, M. Bernardi, *Mol. Phys.* 19 (1970) 553–566.
- [60] B.H. Besler, K.M. Merz, P.A. Kollman, *J. Comput. Chem.* 11 (1990) 431–439.
- [61] Y. Zhao, D.G. Truhlar, *Theor. Chem. Acc.* 120 (2008) 215–241.
- [62] R. Ditchfield, W.J. Hehre, J.A. Pople, *J. Chem. Phys.* 54 (1971) 724–728.
- [63] M.J. Frisch, G.W. Trucks, H.B. Schlegel, G.E. Scuseria, M.A. Robb, J.R. Cheeseman, G. Scalmani, V. Barone, B. Mennucci, G.A. Petersson, H. Nakatsuji, M. Caricato, X. Li, H.P. Hratchian, A.F. Izmaylov, J. Bloino, G. Zheng, J.L. Sonnenberg, M. Hada, M. Ehara, K. Toyota, R. Fukuda, J. Hasegawa, M. Ishida, T. Nakajima, Y. Honda, O. Kitao, H. Nakai, T. Vreven, J.A. Montgomery Jr., J.E. Peralta, F. Ogliaro, M. Bearpark, J.J. Heyd, E. Brothers, K.N. Kudin, V.N. Staroverov, T. Keith, R. Kobayashi, J. Normand, K. Raghavachari, A. Rendell, J.C. Burant, S.S. Iyengar, J. Tomasi, M. Cossi, N. Rega, J.M. Millam, M. Klene, J.E. Knox, J.B. Cross, V. Bakken, C. Adamo, J. Jaramillo, R. Gomperts, R.E. Stratmann, O. Yazyev, A.J. Austin, R. Cammi, C. Pomelli, J.W. Ochterski, R.L. Martin, K. Morokuma, V.G. Zakrzewski, G.A. Voth, P. Salvador, J.J. Dannenberg, S. Dapprich, A.D. Daniels, O. Farkas, J.B. Foresman, J.V. Ortiz, J. Cioslowski, D.J. Fox, *Gaussian 09, Revision B.01*, Gaussian, Inc., Wallingford CT, 2010.
- [64] A. Sikorski, K. Kowalska, K. Krzymiński, J. Błażejowski, *Acta Cryst. E*63 (2007) o2670–o2672.
- [65] B. Zadykiewicz, M. Wera, A. Sikorski, J. Błażejowski, *Acta Cryst. E*65 (2009) o30–o31.
- [66] K. Krzymiński, D. Trzybiński, A. Sikorski, J. Błażejowski, *Acta Cryst. E*65 (2009) o789–o790.
- [67] D. Trzybiński, K. Krzymiński, J. Błażejowski, *Acta Cryst. E*67 (2011) o3205–o3206.
- [68] D. Cremer, J.A. Pople, *J. Am. Chem. Soc.* 97 (1975) 1354–1358.
- [69] S.K. Seth, D. Sarkar, A. Roy, T. Kar, *CrystEngComm* 13 (2011) 6728–6741.
- [70] S.K. Seth, *J. Mol. Struct.* 1070 (2014) 65–74.
- [71] P. Manna, S.K. Seth, A. Das, J. Hemming, R. Prendergast, M. Helliwell, S.R. Choudhury, A. Frontera, S. Mukhopadhyay, *Inorg. Chem.* 51 (2012) 3557–3571.
- [72] S.K. Seth, *J. Mol. Struct.* 1064 (2014) 70–75.
- [73] K. Krzymiński, P. Malecha, P. Storonik, B. Zadykiewicz, J. Błażejowski, *J. Therm. Anal. Calorim.* 100 (2010) 207–214.
- [74] B. Zadykiewicz, K. Krzymiński, P. Storonik, J. Błażejowski, *J. Therm. Anal. Calorim.* 101 (2010) 429–437.

Table captions**Table 1** Crystal data and structural refinement**Table 2** Hydrogen bonds (Å, °)**Table 3** π - π contacts (Å, °)**Table 4** S-O $\cdots\pi$ and C-F $\cdots\pi$ interactions (Å, °)**Table 5** Theoretical lattice energies (E_L) calculated using CRYSTAL09 and contributions to the lattice energies: E_c (cohesive energy calculated from the difference in electronic and nuclear repulsion energy of bulk crystal and molecules in the bulk), $E(D^*)$ (dispersive contribution derived from modified Grimme model), E_{BSSE} (basis set superposition error energy correction) and ESP fitted atomic partial charges on N10 atom of the acridine/acridinium derivatives. All energies values in kJ mol^{-1} .

Figure captions

Scheme 1 Canonical structures of the compounds investigated; **1** – 9-methylacridine, **2** – 9-ethylacridine, **3** – 9-(bromomethyl)acridine monohydrate, **4** – 9-piperidin-1-ylacridine, **5** – 10-methyl-9-vinylacridinium trifluoromethanesulphonate, **6** – 9-(bromomethyl)-10-methylacridinium trifluoromethanesulphonate, **7** – 10-methyl-9-phenyl-acridinium trifluoromethanesulphonate

Scheme 2 Ring label and atom numbering scheme

Fig. 1 The molecular structure of compounds **1–7** (25% probability level ellipsoids represent non-H atoms; small spheres of arbitrary radius represent H atoms) showing the labelling of atoms, the numbering of aromatic ring centroids and O–H \cdots O, O–H \cdots N and C–H \cdots O (dashed lines) and S–O \cdots π and C–F \cdots π (dotted lines) interactions

Fig. 2 The intermolecular in the crystal lattice of compounds investigated (see Tables 2–4 for details) (non-H atoms are represented by 25% probability level ellipsoids; H atoms not involved in interactions have been omitted, those involved in interactions are shown as small spheres of arbitrary radius). The O–H \cdots O, O–H \cdots N, C–H \cdots O and C–H \cdots π interactions are represented by dashed lines; $\pi\cdots\pi$, S–O \cdots π and C–F \cdots π are represented by dotted lines

Fig. 3 The supramolecular arrangement of acridine (acridinium cation) moieties in the crystal structures

Fig. 4 Layers of cations and anions in the crystal structure of **5**, **6** and **7**

Fig. 5 The Hirshfeld surface (front (left) and reverse (right) views) of the acridine and acridinium cation moieties reflecting the normalized contact distance (d_{norm}) with selected interactions listed in Tables 2–4

Fig. 6 Comparison of full fingerprint plots of acridine and acridinium cation moieties of compounds investigated

Fig. 7 The percentage contributions of various close intermolecular contacts to the Hirshfeld surface area. Other contacts constitute: **(3A)** C \cdots N, N \cdots C, C \cdots Br, Br \cdots Br, Br \cdots O; **(3B)** , C \cdots N, N \cdots C, C \cdots Br, Br \cdots C, Br \cdots Br, Br \cdots O; **(4)** C \cdots N, N \cdots C; **(5)** N \cdots O, N \cdots F, N \cdots S, C \cdots S; **(6A and 6B)** Br \cdots F, Br \cdots Br, N \cdots O, C \cdots N, N \cdots C; **(7)** C \cdots N, N \cdots C, N \cdots O

Table 1 Crystal data and structural refinement

Experimental details	1	2	3	4	5	6	7
Empirical formula	C ₁₄ H ₁₃ N	C ₁₅ H ₁₃ N	C ₁₄ H ₁₀ NBr·H ₂ O	C ₁₄ H ₁₄ N ₂	C ₁₄ H ₁₄ N·CF ₃ SO ₂	C ₁₅ H ₁₃ NBr·CF ₃ SO ₂	C ₂₀ H ₁₈ N·CF ₃ SO ₂
Formula weight	193.24	207.26	290.16	262.34	369.35	436.24	419.41
Temperature [K]	295(2)	295(2)	295(2)	295(2)	295(2)	295(2)	295(2)
Wavelength	1.54184	1.54184	1.54184	1.54184	1.54184	1.54184	1.54184
Crystal system, space group	Orthorhombic, P 2 ₁ 2 ₁ 2 ₁	Monoclinic, P 2 ₁ /c	Orthorhombic, P 2 ₁ 2 ₁ 2 ₁	Triclinic, P-1	Monoclinic, P 2 ₁ /n	Triclinic, P-1	Monoclinic, P 2 ₁ /n
Unit cell dimensions [Å, °]	a = 6.8716(3) b = 11.2769(5) c = 13.1594(7)	a = 17.0354(3) b = 9.45596(12) β = 115.476(2) c = 15.6179(3)	a = 4.76180(4) b = 16.10280(12) c = 31.7756(2)	a = 7.1506(3) α = 70.461(4) b = 9.9307(4) β = 86.742(3) c = 11.3298(4) γ = 69.887(4)	a = 9.6193(3) b = 13.0378(3) β = 101.766(3) c = 13.2859(4)	a = 11.4473(6) α = 101.023(4) b = 11.7778(7) β = 93.300(4) c = 13.6223(6) γ = 112.071(5)	a = 9.6457(2) b = 12.5613(2) β = 105.642(2) c = 16.1104(3)
Volume [Å ³]	1019.73(8)	2271.20(8)	2436.50(3)	710.43(6)	1631.23(8)	1653.63(16)	1879.69(6)
Z, Calculated density [Mg/m ³]	4, 1.259	8, 1.212	8, 1.582	2, 1.226	4, 1.504	4, 1.752	4, 1.482
Absorption coeff. μ [mm ⁻¹]	0.564	0.539	4.447	0.556	2.228	5.030	2.010
F(000)	408	880	1168	280	760	872	864
Crystal description, colour	Plate, white	Block, white	Plate, yellow	Prism, orange	Needle, yellow	Plate, yellow	Plate, yellow
Crystal size [mm]	0.83 x 0.46 x 0.14	0.73 x 0.68 x 0.57	0.63 x 0.23 x 0.15	0.73 x 0.53 x 0.34	0.52 x 0.17 x 0.15	0.25 x 0.22 x 0.085	0.55 x 0.20 x 0.10
θ range for data collection [°]	5.17–67.24	5.49–67.32	3.91–67.53	6.79–67.43	4.80–67.55	3.34–67.48	4.53–67.31
Limiting indices	-8<h<=5, -11<k<=13, -14<l<=15	-20<h<=20, -11<k<=11, -18<l<=16	-5<h<=5, -19<k<=19, -38<l<=38	-8<h<=8, -11<k<=11, -13<l<=13	-11<h<=11, -13<k<=15, -15<l<=15	-13<h<=12, -14<k<=14, -16<l<=15	-11<h<=11, -15<k<=14, -19<l<=19
Reflections collected / unique	2987 / 1611 [R _{int} = 2.26%]	39777 / 4069 [R _{int} = 2.91%]	56027 / 4393 [R _{int} = 4.13%]	13166 / 2523 [R _{int} = 7.91%]	18269 / 2942 [R _{int} = 3.53%]	19923 / 5903 [R _{int} = 4.85%]	11770 / 3358 [R _{int} = 2.78%]
Completeness 2θ = 67.684	98.4%	99.0%	99.5%	98.2%	99.5%	98.6%	98.8%
Absorption correction	Semi-empirical from equivalents	Semi-empirical from equivalents	Semi-empirical from equivalents	Semi-empirical from equivalents	Semi-empirical from equivalents	Semi-empirical from equivalents	Semi-empirical from equivalents
T _{min} , T _{max}	0.953, 0.726	0.978, 0.404	0.987, 0.307	0.853, 0.742	0.983, 0.703	0.983, 0.703	0.823, 0.642
Refinement method	Full-matrix least-squares on F ²	Full-matrix least-squares on F ²	Full-matrix least-squares on F ²	Full-matrix least-squares on F ²	Full-matrix least-squares on F ²	Full-matrix least-squares on F ²	Full-matrix least-squares on F ²
Data / restraints / parameters	1611 / 0 / 138	4069 / 0 / 292	4393 / 0 / 320	2523 / 0 / 190	2942 / 0 / 228	5903 / 0 / 453	3358 / 0 / 264
Goodness-of-fit on [F] ²	1.045	1.017	1.049	1.050	1.035	1.018	1.033
Final R indices [I>2 σ (I)]	R ₁ = 3.60%, wR ₂ = 9.80%	R ₁ = 3.84%, wR ₂ = 10.79%	R ₁ = 2.28%, wR ₂ = 6.52%	R ₁ = 5.37%, wR ₂ = 15.49%	R ₁ = 4.14%, wR ₂ = 11.37%	R ₁ = 5.01%, wR ₂ = 12.85%	R ₁ = 4.34%, wR ₂ = 11.75%
R indices (all data)	R ₁ = 4.02%, wR ₂ = 10.36%	R ₁ = 4.28%, wR ₂ = 11.27%	R ₁ = 2.31%, wR ₂ = 6.55%	R ₁ = 5.68%, wR ₂ = 16.06%	R ₁ = 4.82%, wR ₂ = 12.12%	R ₁ = 6.57%, wR ₂ = 14.42%	R ₁ = 4.96%, wR ₂ = 12.33%
Δρ _{max} , Δρ _{min} (e Å ⁻³)	0.131, -0.105	0.125, -0.103	0.212, -0.351	0.206, -0.183	0.190, -0.293	1.234, -0.689	0.333, -0.266
CCDC number	1058686	1058685	1058682	1058683	1058684	1058681	1058687

Table 2 Hydrogen bonds (Å, °)

	D–H…A	D–H	H…A	D…A	D–H…A	Symmetry codes
2	C1B–H1B…Cg1B	0.93	2.98	3.738(2)	139	$-x + 1, y - \frac{1}{2}, -z + \frac{1}{2}$ (i)
3	O1C–H1C…N10A	0.84(4)	2.01(5)	2.857(4)	179(6)	x, y, z
	O1D–H1D…N10B	0.86(4)	1.99(4)	2.848(4)	174(5)	x, y, z
	O1C–H2C…O1D	0.85(4)	1.88(4)	2.733(4)	175(5)	$x + 1, y, z$ (i)
	O1D–H2D…O1C	0.85(4)	1.90(4)	2.727(4)	163(4)	x, y, z
	C1B–H1B…O1C	0.93	2.47	3.351(4)	158	$-x + 1, y - \frac{1}{2}, -z + 1\frac{1}{2}$ (ii)
4	C19–H19A…Cg2	0.97	2.76	3.650(2)	153	$x + 1, y, z$ (i)
5	C5–H5…O1	0.93	2.49	3.275(3)	142	x, y, z
6	C1B–H1B…O2B	0.93	2.53	3.458(5)	174	$-x, -y + 2, -z + 1$ (i)
	C3A–H3A…O1B	0.93	2.59	3.446(7)	154	$-x + 1, -y + 2, -z + 2$ (ii)
	C15B–H15C…O1A	0.97	2.40	3.338(6)	163	$x, y + 1, z$ (iii)
	C15B–H15D…O2B	0.97	2.57	3.395(5)	144	$-x, -y + 2, -z + 1$ (i)
	C17A–H17C…O2B	0.96	2.56	3.353(6)	140	$x + 1, y, z$ (iv)
7	C4–H4…O3	0.93	2.58	3.483(3)	165	$-x + 1\frac{1}{2}, y - \frac{1}{2}, -z + 1\frac{1}{2}$ (i)
	C5–H5…O1	0.93	2.35	3.205(3)	152	x, y, z
	C21–H21B…O1	0.96	2.55	3.461(3)	158	x, y, z

Table 3 π - π contacts (\AA , $^\circ$)

	<i>Cg</i> _I	<i>Cg</i> _J	<i>Cg</i> _I ... <i>Cg</i> _J	Dihedral angle	Interplanar distance	Offset	Symmetry codes	
1	2	3	3.981(1)	1.8(1)	3.562(1)	1.778(1)	$x - 1, y, z$ (i)	
	3	2	3.981(1)	1.8(1)	3.561(1)	1.780(1)	$x + 1, y, z$ (ii)	
2	1A	3A	3.952(1)	0.3(1)	3.518(1)	1.801(1)	$-x, -y + 1, -z$ (ii)	
	3A	1A	3.952(1)	0.3(1)	3.513(1)	1.810(1)	$-x, -y + 1, -z$ (ii)	
	1B	3B	3.781(1)	0.5(1)	3.500(1)	1.430(1)	$-x + 1, -y, -z + 1$ (iii)	
3	3B	1B	3.781(1)	0.5(1)	3.503(1)	1.423(1)	$-x + 1, -y, -z + 1$ (iii)	
	1A	2A	3.688(2)	0.6(1)	3.408(1)	1.410(1)	$x + 1, y, z$ (i)	
	2A	1A	3.689(2)	0.6(1)	3.421(1)	1.380(1)	$x - 1, y, z$ (iii)	
4	1A	3A	3.735(2)	1.3(1)	3.444(1)	1.445(1)	$x - 1, y, z$ (iii)	
	3A	1A	3.735(2)	1.3(1)	3.421(1)	1.499(1)	$x + 1, y, z$ (i)	
	2A	3A	4.057(2)	1.9(2)	3.454(1)	2.128(1)	$x - 1, y, z$ (iii)	
	3A	2A	4.057(2)	1.9(1)	3.404(1)	2.207(1)	$x + 1, y, z$ (i)	
	1B	2B	3.639(2)	1.2(1)	3.409(1)	1.273(1)	$x - 1, y, z$ (iii)	
	2B	1B	3.639(2)	1.2(1)	3.416(1)	1.254(1)	$x + 1, y, z$ (i)	
	1B	3B	3.712(2)	0.6(2)	3.464(1)	1.334(1)	$x - 1, y, z$ (iii)	
	3B	1B	3.713(2)	0.6(2)	3.452(1)	1.368(1)	$x + 1, y, z$ (i)	
	2B	3B	3.991(2)	1.3(2)	3.431(1)	2.039(1)	$x - 1, y, z$ (iii)	
	3B	2B	3.991(2)	1.3(2)	3.466(1)	1.979(1)	$x + 1, y, z$ (i)	
	4	1	1	3.946(1)	0.0(6)	3.526(1)	1.772(1)	$x + 1, y, z$ (ii)
	5	1	2	3.768(1)	2.5(6)	3.506(1)	1.381(1)	$-x + 1, -y + 2, -z + 1$ (ii)
2		1	3.768(1)	2.5(6)	3.562(1)	1.229(1)	$-x + 1, -y + 2, -z + 1$ (ii)	
2		3	3.906(1)	4.1(7)	3.601(1)	1.513(1)	$-x + 1, -y + 2, -z + 1$ (ii)	
3		2	3.906(1)	4.1(7)	3.528(1)	1.676(1)	$-x + 1, -y + 2, -z + 1$ (ii)	
6	2	2	3.917(1)	0.0(1)	3.393(1)	1.957(1)	$-x + 1, -y + 1, -z$ (i)	
	1A	3B	4.008(3)	3.0(2)	3.553(2)	1.855(1)	x, y, z	
	3B	1A	4.008(3)	3.0(2)	3.612(2)	1.737(1)	x, y, z	
	3A	1B	3.882(3)	5.4(2)	3.573(2)	1.518(1)	x, y, z	
	1B	3A	3.882(3)	5.4(2)	3.422(2)	1.833(1)	x, y, z	
	3A	3B	3.794(3)	2.4(2)	3.550(2)	1.339(1)	x, y, z	
	3B	3A	3.793(3)	2.4(2)	3.574(2)	1.270(1)	x, y, z	
7	1	3	3.659(1)	4.2(1)	3.568(1)	0.811(1)	$x - 2, -y + 1, -z + 1$ (ii)	
	3	1	3.659(1)	4.2(1)	3.540(1)	0.926(1)	$x - 2, -y + 1, -z + 1$ (ii)	
	3	4	4.036(1)	17.9(1)	3.442(1)	2.108(1)	$-x + 1\frac{1}{2}, y + \frac{1}{2}, -z + \frac{1}{2}$ (iii)	
	4	3	4.036(1)	17.9(1)	3.769(1)	1.444(1)	$-x + 1\frac{1}{2}, y - \frac{1}{2}, -z + \frac{1}{2}$ (iv)	

*Cg*₁ is the centroid of the C₉/N₁₀/C₁₁-C₁₂/ C₁₃-C₁₄ ring

*Cg*_{1A} is the centroid of the C_{9A}/N_{10A}/C_{11A}-C_{12A}/ C_{13A}-C_{14A} ring

*Cg*_{1B} is the centroid of the C_{9B}/N_{10B}/C_{11B}-C_{12B}/ C_{13B}-C_{14B} ring

*Cg*₂ is the centroid of the C₁-C₄/ C₁₁-C₁₂ ring

*Cg*_{2A} is the centroid of the C_{1A}-C_{4A}/ C_{11A}-C_{12A} ring

*Cg*_{2B} is the centroid of the C_{1B}-C_{4B}/ C_{11B}-C_{12B} ring

*Cg*₃ is the centroid of the C₅-C₈/ C₁₃-C₁₄ ring

*Cg*_{3A} is the centroid of the C_{5A}-C_{8A}/ C_{13A}-C_{14A} ring

*Cg*_{3B} is the centroid of the C_{5B}-C_{8B}/ C_{13B}-C_{14B} ring

*Cg*₄ is the centroid of the C₁₅-C₂₀ ring

*Cg*_I...*Cg*_J is the distance between ring centroids.

The dihedral angle is that between the planes of the rings I and J.

Interplanar distance is the perpendicular distance of *Cg*_I from ring J.

Offset is the distance between *Cg*_I and the perpendicular projection of *Cg*_J on ring I

Table 4 S–O⋯π and C–F⋯π interactions (Å, °)

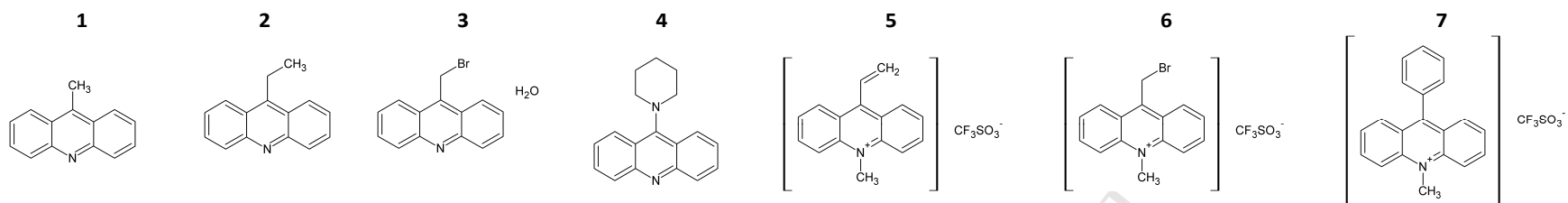
	Y	X	Cg	X⋯Cg	Y⋯Cg	Y–X⋯Cg	Symmetry codes
5	C18	F2	Cg1	3.427(2)	4.308(2)	123.9(2)	$x - \frac{1}{2}, -y + \frac{1}{2}, z + \frac{1}{2}$ (ii)
	C18	F2	Cg3	3.685(2)	4.147(2)	101.0(2)	$x - \frac{1}{2}, -y + \frac{1}{2}, z + \frac{1}{2}$ (ii)
	C18	F3	Cg3	3.670(2)	4.147(2)	101.7(2)	$x + \frac{1}{2}, -y + \frac{1}{2}, z + \frac{1}{2}$ (ii)
	S1	O1	Cg1	3.825(2)	3.801(2)	78.3(2)	$x + \frac{1}{2}, -y + \frac{1}{2}, z + \frac{1}{2}$ (iii)
	S1	O1	Cg2	3.872(2)	4.652(2)	114.7(2)	$x + \frac{1}{2}, -y + \frac{1}{2}, z + \frac{1}{2}$ (iii)
	S1	O2	Cg1	3.679(2)	3.801(2)	83.9(2)	$x + \frac{1}{2}, -y + \frac{1}{2}, z + \frac{1}{2}$ (iii)
	S1	O2	Cg3	3.847(2)	4.411(2)	103.9(2)	$x + \frac{1}{2}, -y + \frac{1}{2}, z + \frac{1}{2}$ (iii)
	S1	O3	Cg1	3.755(2)	3.801(2)	81.0(2)	$x + \frac{1}{2}, -y + \frac{1}{2}, z + \frac{1}{2}$ (iii)
6	C18B	F3A	Cg2A	3.437(4)	4.547(5)	140.4(4)	x, y, z
	S1A	O2A	Cg1A	3.410(5)	3.879(2)	97.6(2)	x, y, z
	S1B	O2B	Cg1B	3.530(4)	3.671(2)	84.1(2)	x, y, z
	S1B	O2B	Cg2B	3.401(4)	4.383(2)	125.0(2)	x, y, z
	S1A	O3A	Cg1A	3.271(5)	3.879(2)	104.0(2)	x, y, z
	S1B	O3B	Cg1B	3.666(5)	3.671(2)	78.9(2)	x, y, z
	S1	O3	Cg1	3.552(2)	4.949(2)	174.2(2)	$x + \frac{1}{2}, -y + 1\frac{1}{2}, z + \frac{1}{2}$ (v)

Cg1 is the centroid of the C9/N10/C11–C12/ C13–C14 ring
 Cg1A is the centroid of the C9A/N10A/C11A–C12A/ C13A–C14A ring
 Cg1B is the centroid of the C9B/N10B/C11B–C12B/ C13B–C14B ring
 Cg2 is the centroid of the C1–C4/ C11–C12 ring
 Cg2A is the centroid of the C1A–C4A/ C11A–C12A ring
 Cg2B is the centroid of the C1B–C4B/ C11B–C12B ring
 Cg3 is the centroid of the C5–C8/ C13–C14 ring
 Cg3A is the centroid of the C5A–C8A/ C13A–C14A ring
 Cg3B is the centroid of the C5B–C8B/ C13B–C14B ring
 Cg4 is the centroid of the C15–C20 ring

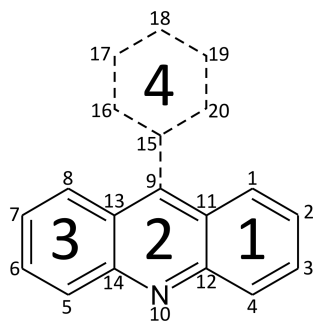
Table 5 Theoretical lattice energies (E_L) calculated using CRYSTAL09 and contributions to the lattice energies: E_c (cohesive energy calculated from the difference in electronic and nuclear repulsion energy of bulk crystal and molecules in the bulk), $E(D^*)$ (dispersive contribution derived from modified Grimme model), E_{BSSE} (basis set superposition error energy correction) and ESP fitted atomic partial charges on N10 atom of the acridine/acridinium derivatives. All energies values in kJ mol^{-1} .

Compound no	E_c	$E(D^*)$	$E_L = E_c + E(D^*) + E_{BSSE}$	Atomic partial charges on N10 atom
1	-18.6	-116.9	-131.6	-0.8069 ^a
2	-12.3	-122.5	-133.1	-0.7766 (N10A) ^a -0.6253 (N10B) ^a
3	-139.4	-151.1	-227.6	-0.2546 (N10A) ^a -0.1789 (N10B) ^a -0.8082 (N10A) ^b -0.8097 (N10B) ^b
4	-6.9	-148.1	-151.4	-0.7710 (N10A) ^a
5	-448.8	-176.6	-530.6	-0.0252 ^a +0.0219 ^b
6	-446.1	-192.6	-541.9	-0.0804 (N10A) ^a -0.3543 (N10B) ^a -0.2358 (N10A) ^b -0.2358 (N10B) ^b
7	-431.9	-202.0	-535.8	-0.1504 ^a -0.2425 ^b

^a Atomic partial charges calculated at the M06-2X/6-31++G** level for all atoms of the electroneutral asymmetric unit;
^b Atomic partial charges calculated at the M06-2X/6-31++G** level separately for molecules in the unit cell (assuming charge +1 for acridinium molecule and -1 for trifluoromethanesulfonate counterpart)



Scheme 1 Canonical structures of the compounds investigated; **1** – 9-methylacridine, **2** – 9-ethylacridine, **3** – 9-(bromomethyl)acridine monohydrate, **4** – 9-piperidin-1-ylacridine, **5** – 10-methyl-9-vinylacridinium trifluoromethanesulphonate, **6** – 9-(bromomethyl)-10-methylacridinium trifluoromethanesulphonate, **7** – 10-methyl-9-phenyl-acridinium trifluoromethanesulphonate



Scheme 2 Ring label and atom numbering scheme

ACCEPTED MANUSCRIPT

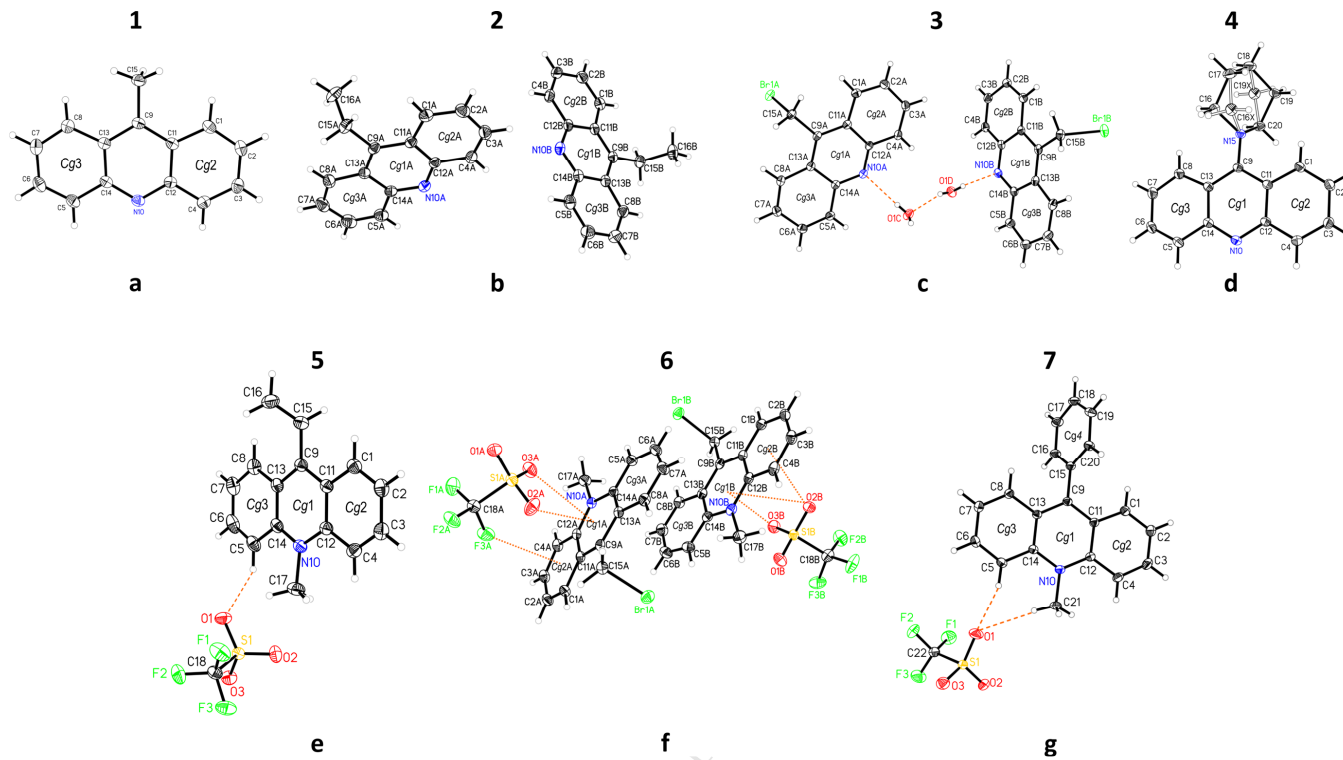


Fig. 1 The asymmetric unit of compounds **1–7** (25% probability level ellipsoids represent non-H atoms; small spheres of arbitrary radius represent H atoms) showing the labelling of atoms, the numbering of aromatic ring centroids and O–H···O, O–H···N and C–H···O (dashed lines) and S–O··· π and C–F··· π (dotted lines) interactions

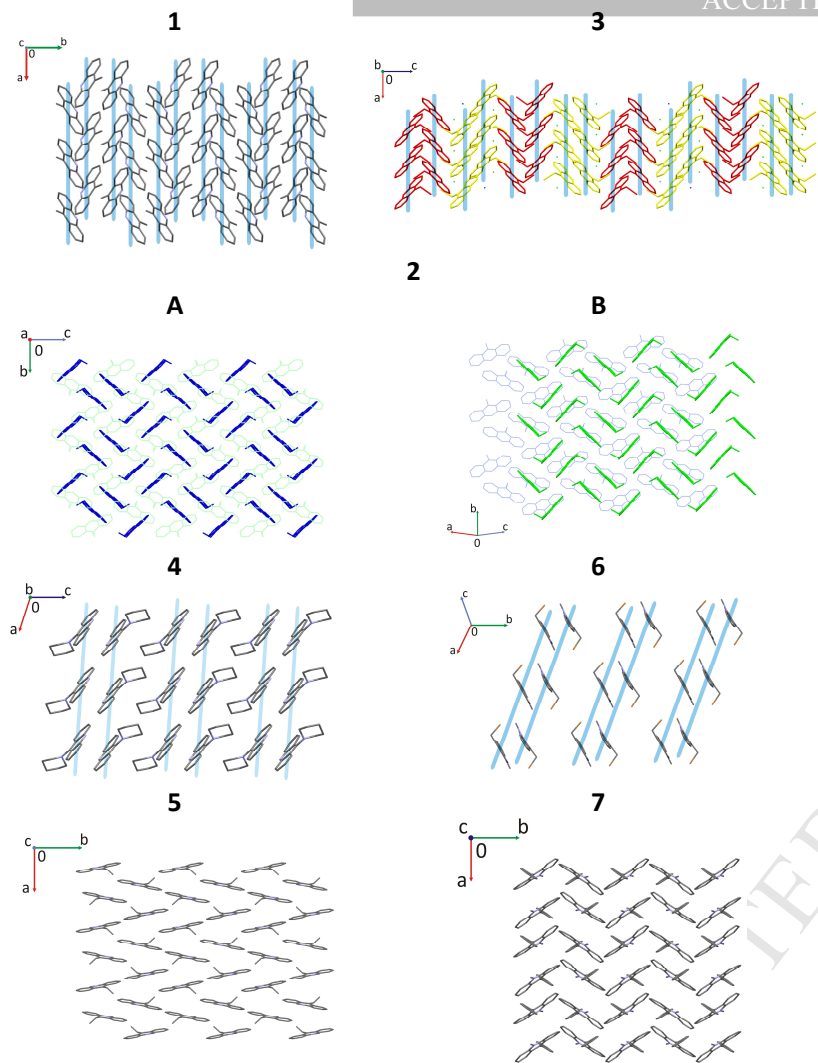


Fig. 3 The supramolecular arrangement of acridine (acridinium cation) moieties in the crystal structures

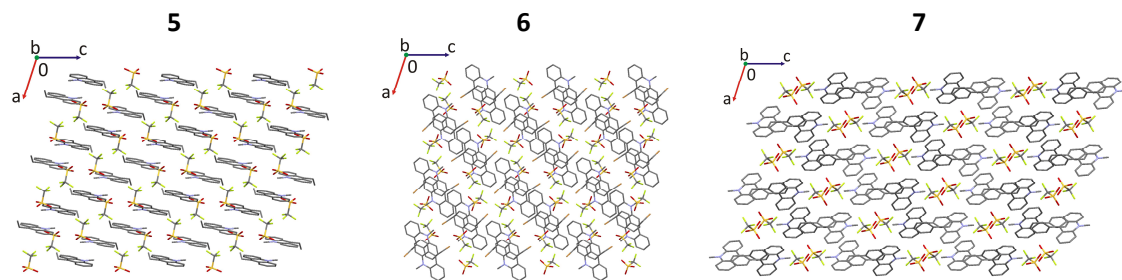


Fig. 4 Layers of cations and anions in the crystal structure of **5**, **6** and **7**

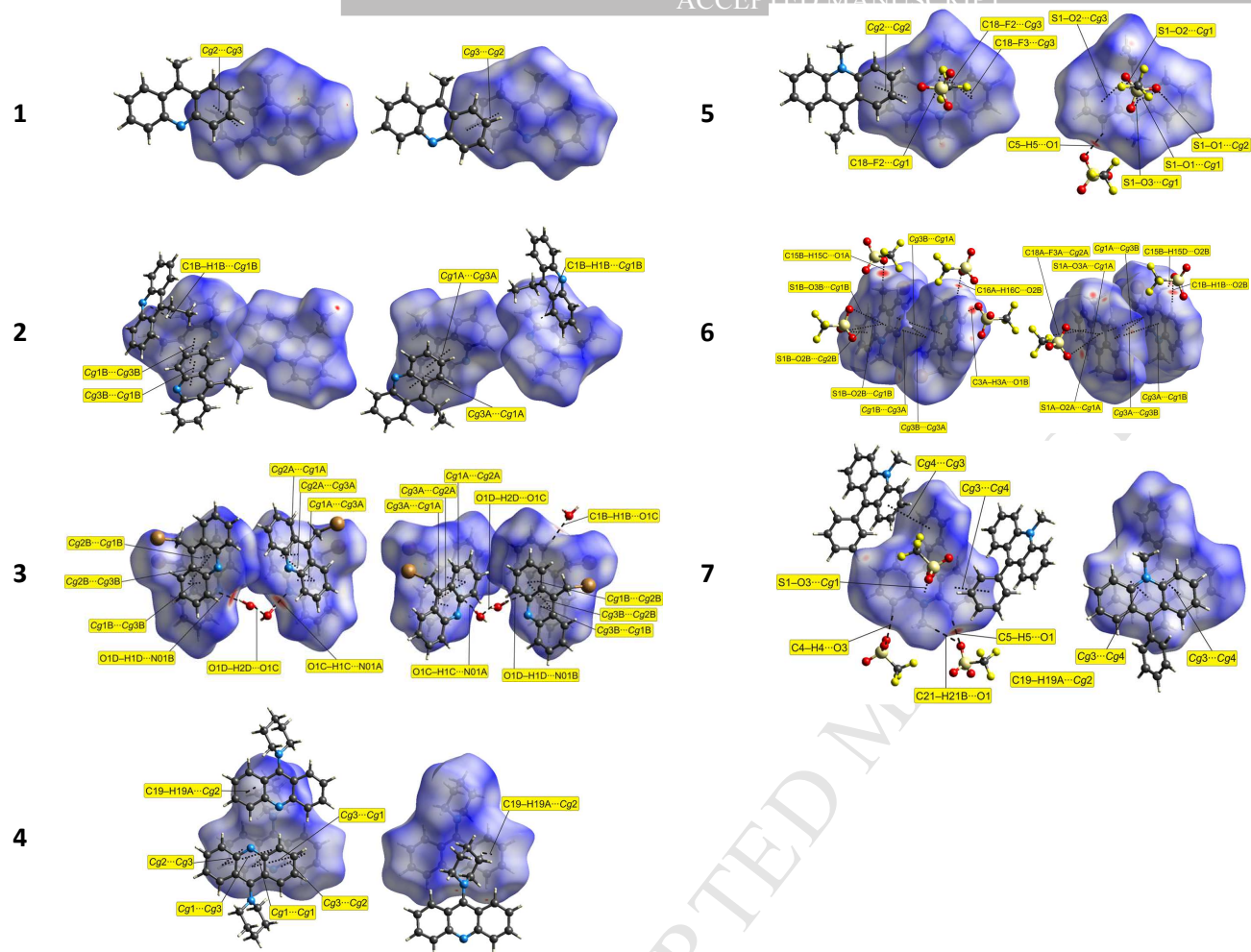


Fig. 5 The Hirshfeld surface (front (left) and reverse (right) views) of the acridine and acridinium cation moieties reflecting the normalized contact distance (d_{norm}) with selected interactions listed in Tables 2–4

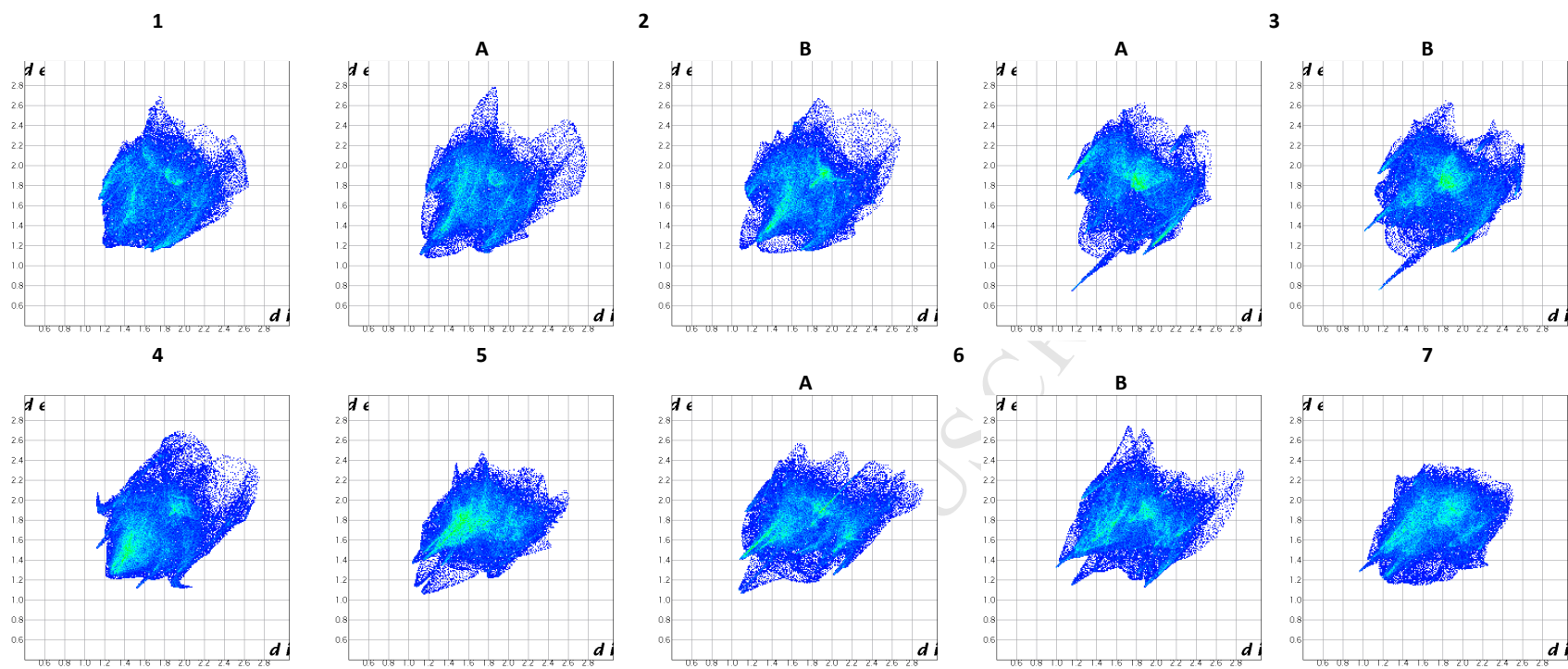


Fig. 6 Comparison of full fingerprint plots of acridine and acridinium cation moieties of compounds investigated

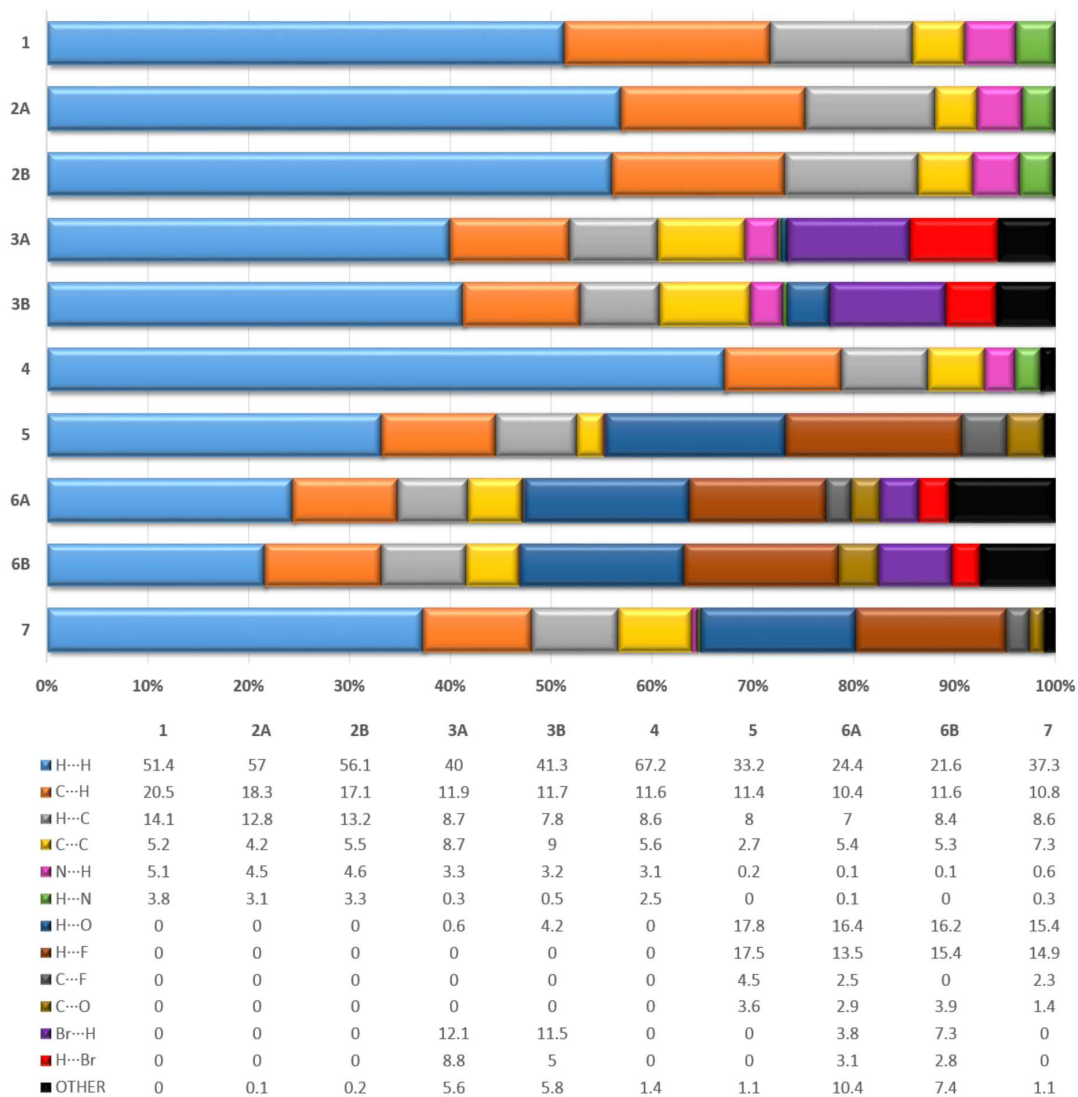


Fig. 7 The percentage contributions of various close intermolecular contacts to the Hirshfeld surface area. Other contacts constitute: **(3A)** C...N, N...C, C...Br, Br...Br, Br...O; **(3B)** C...N, N...C, C...Br, Br...C, Br...Br, Br...O; **(4)** C...N, N...C; **(5)** N...O, N...F, N...S, C...S; **(6A and 6B)** Br...F, Br...Br, N...O, C...N, N...C; **(7)** C...N, N...C, N...O

Highlights

- A series of 9-substituted acridine and their N-methylated salts were synthesized.
- Single crystal X-ray diffraction analysis of the compounds was achieved.
- The intermolecular interactions have been analyzed by Hirshfeld surfaces analysis.
- Computational methods were applied to understand the nature of intermolecular interactions.